CONF-911202--28

DE92 005470



[To be published in *Interface Dynamics & Growth*, Proceedings of the 1991 Fall Meeting of the Materials Research Society, Boston, Massachusetts, December 2–6, 1991]



# EPITAXIAL $YBa_2Cu_3O_{7-x}$ THIN FILMS: SCANNING TUNNELING MICROSCOPE STUDY OF THE INITIAL STAGES OF EPITAXIAL GROWTH, GROWTH MECHANISM, AND EFFECTS OF SUBSTRATE TEMPERATURE

Shen Zhu,* Douglas H. Lowndes, X.-Y.Zheng,* David P. Norton,
and
R. J. Warmack





*The University of Tennessee
Knoxville, TN 37996
Solid State Division
Oak Ridge National Laboratory
Oak Ridge, Tennessee 37831-6056
managed by
MARTIN MARIETTA ENERGY SYSTEMS, INC.
for the
U.S. DEPARTMENT OF ENERGY
under contract DE-AC05-84OR21400

# EPITAXIAL $YBa_2Cu_3O_{7-x}$ THIN FILMS: SCANNING TUNNELING MICROSCOPE STUDY OF THE INITIAL STAGES OF EPITAXIAL GROWTH, GROWTH MECHANISM, AND EFFECTS OF SUBSTRATE TEMPERATURE

SHEN ZHU,* DOUGLAS H. LOWNDES,† X.-Y. ZHENG,* DAVID P. NORTON,† AND R. J. WARMACK‡

* Department of Physics and Astronomy, The University of Tennessee, Knoxville, TN 37996

† Solid State Division, Oak Ridge National Laboratory, P.O. Box 2008, Oak Ridge, TN 37831-6056

‡ Health and Safety Research Division, Oak Ridge National Laboratory, Oak Ridge, TN 37831-6123

## ABSTRACT

The surface microstructure of epitaxial $YBa_2Cu_3O_{7-x}$ films grown by pulsed laser ablation on (001) MgO and $SrTiO_3$ substrates has been studied at various growth stages, ranging in thickness from eight *c*-axis perpendicular unit cells to ~220 nm. On MgO (lattice mismatch ~9%) even the thinnest films grow unit cell-by-unit cell by an island growth mechanism. However, on $SrTiO_3$ (mismatch ~1%), a transition from a layer-like growth mode to island growth is observed as the film thickness increases. Islands with clear spiral growth structures are observed in even the thinnest films on MgO, but for films grown on $SrTiO_3$ the spiral growth features are found only for film thicknesses slightly greater than the critical thickness for the switch to an island growth mode. The islands consist of stacks of atomically flat terraces whose step heights are multiples of the *c*-axis lattice parameter. The island density decreases significantly with increasing film thickness, while their diameters range from 50–400 nm, increasing with growth temperature. The terraced island grain morphology causes a surface roughness of from 10 to 30 nm (depending on growth temperature) in films ~200 nm thick.

## INTRODUCTION

The growth mechanism of epitaxial $YBa_2Cu_3O_{7-x}$ (YBCO) films is of interest because the structure and properties of copper oxide superconductors are quite anisotropic, and because very thin, continuous YBCO layers are needed in multilayered device structures and for fundamental studies of high-temperature superconductivity (HTSc) [1,2]. The microstructure of YBCO films is expected to depend on a number of 'primary' experimental parameters, among which are deposition temperature and rate, the epitaxial relationship with the single-crystal substrate, and oxygen pressure, since these parameters already are known to affect their superconducting properties [3]. In this paper, we report results of recent scanning tunneling microscope (STM) studies of the near-surface microstructures that form during the initial stages of epitaxial growth of very thin YBCO films. From these images we have determined the film-growth mechanisms and some of the effects of substrate temperature on film growth.

## EXPERIMENTAL

YBCO thin films were grown on (001) substrates of $SrTiO_3$ (ST) and MgO by KrF (248 nm) excimer laser ablation of a high-density commercial polycrystalline YBCO target. The laser beam was focused to a spot (energy density ~2 $J/cm^2$) on the rotating target and was scanned over the target surface to maintain a nearly constant target morphology [3]. The laser-ablation plasma "plume" was nearly normal to the target surface and to the opposing heater surface, on which the substrates were mounted with silver paint. The chamber was evacuated by a turbopump to $\sim 2 \times 10^{-5}$ Torr prior to deposition. During deposition, the oxygen pressure was constant at 200 mT; after deposition the samples were first cooled 150°C at 10°C/min with the oxygen pressure increasing to 400 T, then cooled at 10°C/min to room temperature. The deposition rate was ~0.05 nm/pulse; at a laser repetition rate of 2.2 Hz the time-averaged film-growth rate was ~0.11 nm/s for all of the samples described here. The range of heater temperatures used was T = 660–860°C (held constant ±2°C), measured by a thermocouple embedded in the center of the substrate heater plate. (For comparison, the surface temperature of Si wafers mounted with silver paint and measured by an infrared thermometer was about 40°C lower.) X-ray diffraction (XRD) measurements show that YBCO films deposited under these conditions on (001) ceramic substrates at temperatures of 720°C or higher grow with the *c*-axis perpendicular ($c_\perp$) to the substrate. The nominal thickness of the thinnest films was calculated from the number of laser shots and the known deposition rate; the thicker films were measured using a Dektak II surface profiler; the YBCO film thickness range used in this study was from ~8 $c_\perp$ unit cells to 220 nm. STM images were obtained using a standard Nanoscope II STM operating in air with 0.3 nA tunneling current and 0.5 V voltage bias. The surface roughness of films was determined from STM line scan profiles. All samples were stored in a desiccator for several days before STM measurements.

## RESULTS

Figure 1 shows images of ~8-cell (9.4 nm) thickness YBCO films grown on MgO and ST at T = 720°C. On MgO, the most prominent feature is the high density of distinct platelets or islands, ~$10^{10}$/cm$^2$. The beginnings of spiral growth features can be found at the top of most of the islands, and some of the islands show clear growth spirals of a half to one turn. The typical island size is ~50 nm. In previous work on thicker films [4,5], these features have been associated with a screw dislocation-mediated growth mechanism, with a screw dislocation at the center of each growth spiral, directed nearly perpendicular to the substrate along the *c*-axis direction. These features also are in agreement with transmission electron microscope (TEM) observations of 12 nm-thick YBCO thin films on MgO [6]. However, the 8-cell-thick film grown on ST has quite different surface morphology, as shown in Fig. 1. It is much smoother, consistent with a layer-like growth mechanism at this early stage of growth. Hardly any distinct islands are observed at the YBCO film surface, and the largest film grains are elongated and much larger than on MgO. (In some other regions of the same film on ST, the elongated grains are absent but the surface remains much smoother than on MgO, and there are no distinct islands anywhere.) Line scans over different areas show that the surface height variation (highest peak to lowest valley) for YBCO on MgO is ~7 nm, about four times larger than on ST.

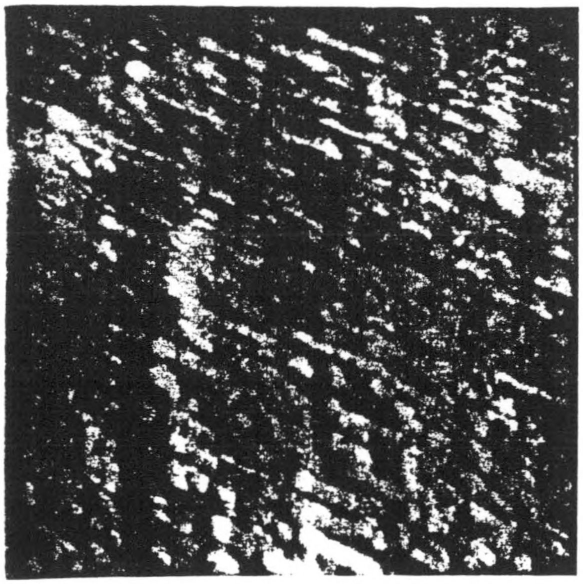

Fig. 1. STM images of $c_\perp$ YBCO films ~8 unit cells thick grown at 720°C on [left] (001) MgO (area: 500 × 500 nm$^2$) and [right] (001) $SrTiO_3$ (area: 1.25 × 1.25 μm$^2$).



The surface morphologies of the ~8-cell-thick YBCO films suggest that possible models for the early stages of film growth are island growth on MgO and layer-like growth on ST [7,8]. An important parameter in considering these two models is the degree of lattice-constant mismatch between YBCO and the two substrates: $a_{MgO}$ = 0.421 nm, $a_{ST}$ = 0.391 nm, $a_{YBCO}$ = 0.382 nm, and $b_{YBCO}$ = 0.389 nm. It is known that YBCO film growth is much more rapid in the *a-b* plane than along the *c*-axis direction. Thus, adatoms on the growing surface will tend to attach to the rapid-growth *a-c* and *b-c* faces, with the film tending to cover the substrate as long as its elastic strain energy does not become too large. However, the large (~9%) lattice mismatch between YBCO and MgO would be expected to drive some type of re-orientation of the YBCO film at an early stage of film growth [8,9]. In fact, a number of low-interfacial energy orientations, differing by rotation of the YBCO in-plane axes about the MgO (001) axis, are predicted by near-coincidence lattice calculations [10,11] and have been observed by XRD in thick YBCO films on MgO [11,12]. Nevertheless, the orientation with the YBCO and MgO in-plane <100> axes aligned seems to be preferred for thick YBCO films grown on well-annealed MgO substrates, despite not being one of the low-strain energy orientations [12]. The fact that the mismatch of YBCO on MgO is much larger than on ST is consistent with our observation that YBCO forms islands at a very early growth stage on MgO, but not on ST.

The layer-like film growth that we observed on ST would be expected to change, with the release of elastic strain energy, when the YBCO film thickens beyond a certain critical thickness that depends on the film's 'primary' elastic conditions and on the conditions of film growth [8,9]. Indeed, as Fig. 2 shows, the surface microstructure of a 16-cell (~19 nm) thick YBCO film grown on ST at T = 720°C consists of numerous islands. The island density in this specimen is similar to that in the 8-cell-thick film on MgO. The islands are nearly circular in projected cross-section and very uniform in size. However, on the top of some of the islands a second layer with rather indistinct shape has just started to nucleate, without the presence of the screw growth features that are so distinct for similar-sized islands on MgO (Fig. 1). At this stage of film growth on ST, it is clear that the ratio of *a-b* plane growth rate to that along the *c*-axis is decreasing, and growth is becoming three-dimensional. In contrast, a 16-cell-thick YBCO film on MgO (Fig. 2) consists of quite well-formed larger islands, some with several growth terraces, others with clear spiral-growth structures, and with edges that are straight segments (rather than round). The existence of multiple terraces provides a number of rapid-growth faces from which the islands can grow laterally.

Figure 1 shows that spiral-growth features are present in the islands of even the thinnest films grown on MgO. In contrast, although a transition from layer-like to island growth occurs around 16 cells thickness for YBCO on ST, we find that these islands do not develop spiral-growth features indicative of screw dislocations at their centers until the film thickness approaches 32 unit cells. Although some screws may originate from the substrate, this observation suggests that many of the screw dislocations present in YBCO films are initiated at island boundaries, when the islands coalesce and overlap (see discussion below).

With increasing film thickness, the surface microstructures of YBCO films grown at 720°C on MgO and ST become similar to each other. The density of islands on both substrates drops to $\sim 10^9/cm^2$ and the size of the largest islands (film grains) is ~400 nm. Figure 3, for 200-nm-thick films, shows that many small islands accompany the growth of a few large islands. Islands that have spiral-shaped growth features at their centers, and strictly layer-like islands, are present in both films. These thicker PLA films are comparable in surface microstructure to sputter-deposited YBCO films [4,5], though the island size in the sputtered films may be ~1.5–2.0 times as large. These observations show that the effect of the film-substrate interaction is submerged in more general growth features after the YBCO film has reached a certain thickness.

However, the film-growth temperature influences the surface microstructure of YBCO films [13], just as it does their superconducting properties [3]. Films grown on ST at or just below 820°C have the highest superconducting critical temperature ($T_c$ ~ 91 K) and critical current density ($J_c$ ~ several $MA/cm^2$ at 77 K). Comparing the images of 16-cell-thick films grown on MgO at 720°C (Fig. 2, right side) and at 820°C (Fig. 4, left side), we see that the small islands of uniform size have been replaced by larger (~400 nm) islands in association with some smaller islands. The large islands in films grown on MgO at 820°C have a layered structure but do not clearly display the spiral-growth feature that appears in the center of most islands grown at low temperatures [4,5,13]. (As noted above, the screw-growth feature only appears at slightly greater thickness in films grown on ST.)

The right side of Fig. 4 shows the initial stages of growth of tilted YBCO layers on a ST substrate that was miscut about 1° away from the (001) plane. (The apparent tilt angle is exaggerated by the high vertical sensitivity and much lower lateral sensitivity of the STM.) Such a substrate provides numerous surface steps on which the rapid-growth *a-c* and *b-c* faces can nucleate and be aligned, resulting in simultaneous growth of many overlapping plates that are epitaxially aligned with the substrate crystal lattice (not the surface normal), apparently overwhelming the spiral growth mechanism [14]. The relationship between the size of the miscut angle and the disappearance of the spiral/island growth features with increasing miscut is described elsewhere [14,15]. In summary, islands are enlarged and the density of screw-growth features decreases at high temperatures, and the use of slightly miscut substrates can entirely eliminate (e.g., on ST or LA) the initial islands and screw-growth features. These trends were confirmed in films grown at 660°C and 860°C.

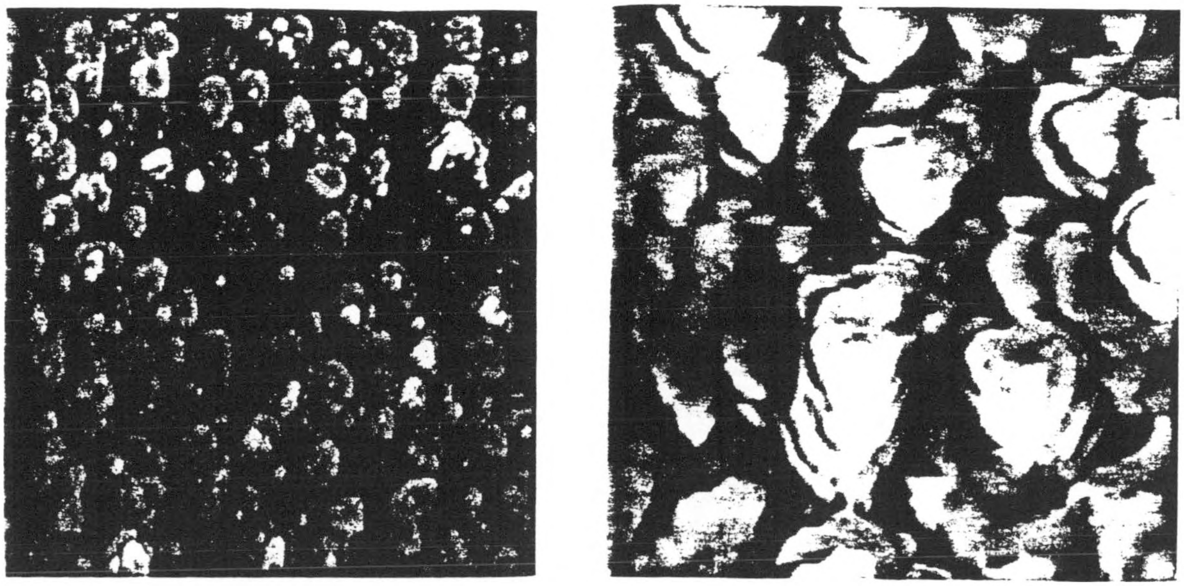

Fig. 2. STM images of $c_\perp$ YBCO films ~16 unit cells thick grown at 720°C on [left] (001) $SrTiO_3$ (area: $1.0 \times 1.0\ \mu m^2$) and [right] (001) MgO (area: $500 \times 500\ nm^2$).

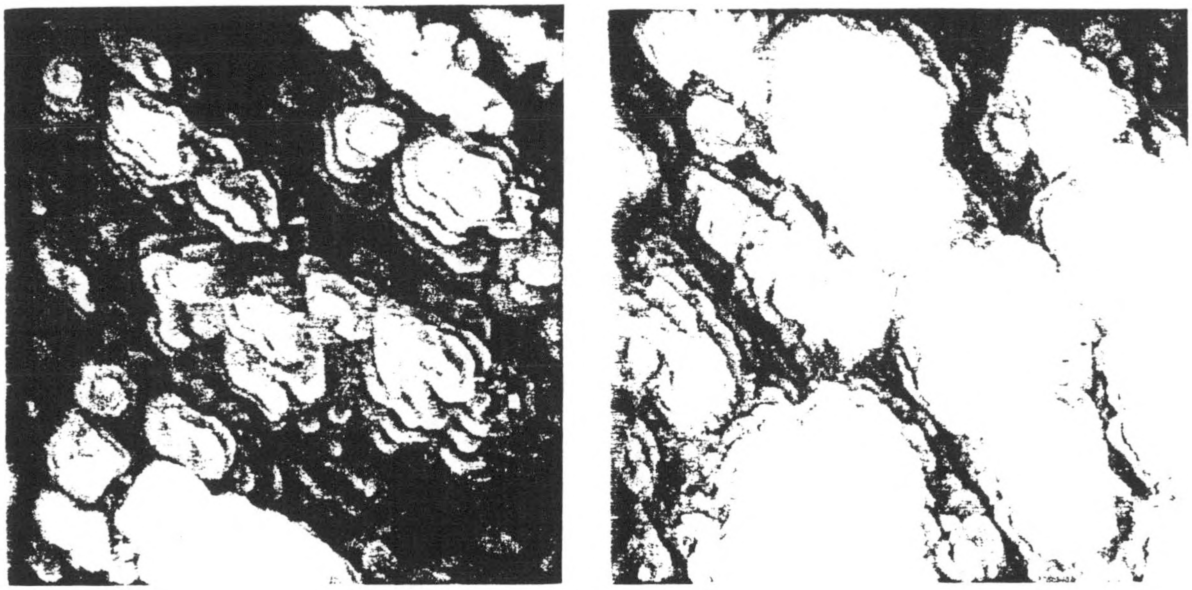

Fig. 3. STM images of $c_\perp$ YBCO films ~200 nm thick grown at 720°C on [left] (001) MgO and [right] (001) $SrTiO_3$ (image areas: $1.0 \times 1.0\ \mu m^2$).



## DISCUSSION

The observation that the density of islands decreases and large islands appear, with increasing growth temperature, is consistent with a strong temperature-dependence of the adatom surface mobility. At low temperatures, adatom mobility is low and sticking coefficients relatively high, so adatoms migrate only short distances and produce a high density of small nuclei for crystal growth. At higher temperatures, however, higher atomic mobility allows adatoms to migrate over a larger surface area, and to find the low-energy, rapid-growth *a-c* and *b-c* faces on islands that already have formed; thus, there is a tendency for more large islands to grow at high temperatures. The density of islands shown in the left side of Fig. 1 (or ideally at

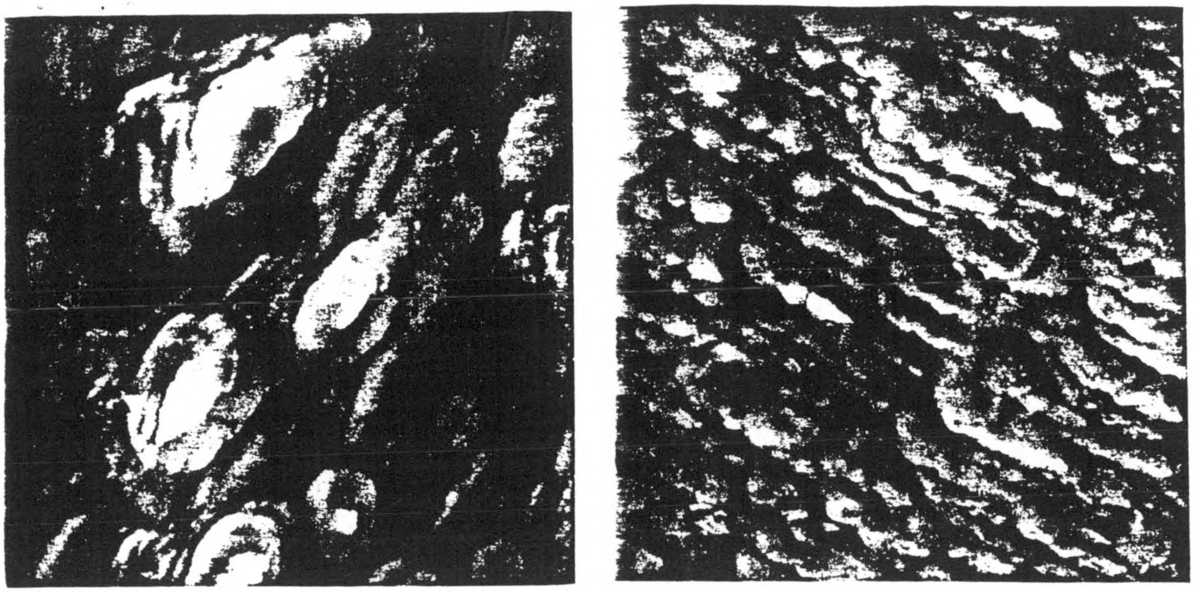

Fig. 4. STM images of $c_\perp$ YBCO films ~16 unit cells thick grown at 820°C on [left] (001) MgO and [right] $SrTiO_3$ miscut ~1° from the (001) plane (image areas: $1.0 \times 1.0\ \mu m^2$).

an even earlier stage) may give an idea of the density of nucleation; the similar size of islands at this stage results from the limited atomic migration and (assumed) uniform surface properties. In the left side of Fig. 4 (820°C), however, the density of islands is reduced and both large and small islands coexist. According to the classical theory of crystal growth [7,16,17] and as shown in Fig. 2 (left side), it is possible for new material to nucleate on top of existing islands. With such increments of film thickness, the islands can grow rapidly laterally from a stack of several terraces. However, each terrace has similar surface condition so that nucleation on terraces can form new islands at locations away from the centers of the underlying islands.

Growth temperature also seems to influence the manner of growth (screw-mediated vs a stack of terraces) of YBCO islands, with fewer screw-mediated islands present at high growth temperatures [13]. Islands with a spiral-growth structure have two obvious elemental characteristics: (1) a continuously evolving faceted grain edge, and (2) a tilted upper face. The reason that screw-mediated islands form is not clear at present. One possibility, for $c_\perp$-oriented YBCO films, is related to lattice mismatch between film and substrate in the *a-b* plane. Calculations [11] based upon the near-coincidence site lattice theory [10] show that a YBCO film can reduce its interfacial energy and maintain a nearly epitaxial relationship with an MgO substrate by growing in any of a number of orientations in which the film's *a-b* plane is rotated about the substrate <001> axis. Many of these orientations have been observed [11,12]. However, a relatively high-energy orientation, with film and substrate <100> axes aligned, seems to be preferred on MgO substrates for which growth steps have been formed on the (001) MgO surface by high-temperature pre-annealing [12]. Studies of the stepped MgO surface [18] and observations of tilted grain boundaries [19] of YBCO on MgO suggest that the tilted top faces may be produced in order to release strain energy built up by the film-substrate epitaxial alignment; this energy is large because of the large lattice misfit between MgO and YBCO. Our studies (Fig. 1) show that strain must be relieved quite early in growth because even an 8-cell-thick film on MgO grows by an island mechanism, rather than the layer-like mode for 8-cell-thick YBCO on ST. In contrast, islands are not seen on ST until the film thickness is ~16 unit cells (Fig. 2), and screw-growth features do not appear on ST until the film thickness is ~32 cells [20]. However, the release of film-substrate (epitaxial) strain energy cannot explain very well the existence of screw dislocations in thick films. Another possibility is that most screw-mediated island growth results from the coalescence of other islands. Because YBCO films contain many growth defects, the height of islands easily can differ by a fraction of a *c*-axis unit cell where they coalesce. Once these islands interconnect, there will be a tilted top face. Adatoms then can extend the original islands and also form a new screw-mediated island; we note that it also should be possible for screw dislocations to terminate at such defects, so that the actual density of screw-growth features contained within a thick film may be much higher than estimated from the surface microstructure. Indeed, our measurements at successive early stages of epitaxial growth suggest that this is true [21].

The fact that YBCO films grow by a terraced island growth mechanism has two direct effects on the morphology of very thin superconducting layers, for example the YBCO layers in $YBa_2Cu_3O_{7-x}/PrBa_2Cu_3O_{7-x}$ (YBCO/PBCO) superlattices. First, if we imagine having grown a PBCO layer with terraced steps on it, then when the laser ablation targets are exchanged to grow the next YBCO layer, it will not be flat but will have steps in it, wherever it crosses the ends of PBCO terraces. We have observed these steps directly by cross-section transmission electron microscopy (TEM) [22,23]. If the YBCO layer is many unit cells thick, then these steps will have little effect on transport properties (e.g., $J_c$), but for one-cell-thick YBCO layers the one-cell steps are a significant barrier to current flow, since the carriers must tunnel along the *c*-axis direction at each such step. Consequently, for one-cell YBCO layers in a PBCO matrix, these steps probably behave as weak links [14,23]. Second, the fact that the islands (grains) in films are higher in the center than at the edges results in undulations in the film's surface height; these undulations increase in amplitude the thicker the film and the higher the growth temperature [13]. Consequently, the individual YBCO layers in ~200 nm thick YBCO/PBCO superlattices are not perfectly flat, but also undulate up and down by ~10–30 nm (depending on growth temperature) over lateral distances of one island/grain diameter (~50–400 nm, depending on growth temperature). These undulations also have been observed by cross-section TEM [23].

This research was sponsored by the Division of Materials Sciences, U.S. Department of Energy under contract DE-AC05-84OR21400 with Martin Marietta Energy Systems, Inc.

## REFERENCES

1. D. H. Lowndes, D. P. Norton, and J. D. Budai, *Phys. Rev. Lett.* **65**, 1160(1990).
2. D. H. Lowndes, D. P. Norton, Shen Zhu, and X.-Y. Zheng, *Proc. of E-MRS Summer School on Laser Ablation of Electronic Materials* (ed. by E. Fogarassy and S. Lazare, Elsevier/North Holland, 1991), in press.
3. D. H. Lowndes, D. P. Norton, J. W. McCamy, R. Feenstra, J. D. Budai, D. K. Christen, and D. B. Poker, *Mat. Res. Soc. Symp. Proc.* **169**, 431 (1990).
4. M. Hawley et al., *Science* **251**, 1587 (1991).
5. C. Gerber et al., *Nature* **350**, 279(1991).
6. M. G. Norton and C. B. Carter, *Physica C,* in press.
7. E. Bauer, Z. Kristallogr, **110**, 372 (1958).
8. R. W. Vook, *Inter. Metals Reviews* **27**, 209 (1982); *Mat. Res. Soc. Symp. Proc.* **103**, 3 (1988).
9. M. H. Grabow and G. H. Gilmer, *Surface Sci.* **194**, 333 (1988); *Mat. Res. Soc. Symp. Proc.* **103**, 13 (1988).
10. R. W. Baluffi, A. Brokman, and A. H. King, *Acta Metall.* **30**, 1453 (1982).
11. D. M. Hwang, T. S. Ravi, R. Ramesh, S.-W. Chan, C. Y. Chen, X. D. Wu, A. Inam, and T. Venkatesan, *Appl. Phys. Lett.* **57**, 1690 (1990).
12. B. H. Moeckly, S. E. Russek, D. K. Lathrop, R. A. Buhrman, J. Li, and J. W. Mayer, *Appl. Phys. Lett.* **57**, 1687 (1990).
13. D. P. Norton, D. H. Lowndes, X.-Y. Zheng, Shen Zhu, and R. J. Warmack, *Phys. Rev. B.* **44**, 9760 (1991).
14. D. H. Lowndes, Shen Zhu, X.-Y. Zheng, and J. D. Budai, submitted for publication; D. H. Lowndes et al., *Proc. Fourth International Symposium on Superconductivity* (Oct. 14–17, 1991, Tokyo, Japan), in press.
15. D. G. Schlom, D. Angelmetti, J. G. Bednorz, R. Broom, A. Catana, T. Frey, Ch. Gerber, H.-J. Guntherodt, H. P. Lang, J. Mannhart, and K. A. Muller, submitted to *Z. Phys. B.*
16. F. C. Frank, *Adv. Phys.* **1**, 93 (1951).
17. W. K. Burton et al., *Philos. Trans. R. Soc. London A* **243**, 299 (1951).
18. P. W. Tasker and D. M. Duffy, *Surf. Sci.*, **137**, 91 (1984).
19. R. Du and C. P. Flynn, *J. Phys.: Condens. Matter* **2**, 1335 (1990).
20. X.-Y. Zheng, D. H. Lowndes, Shen Zhu, and R. J. Warmack, submitted for publication.
21. Shen Zhu, D. H. Lowndes, X.-Y. Zheng, and R. J. Warmack, in preparation.
22. D. H. Lowndes, D. P. Norton, J. D. Budai, S. J. Pennycook, D. K. Christen, B. C. Sales, and R. Feenstra, *Mat. Res. Soc. Symp. Proc.* **191**, 153 (1990).
23. S. J. Pennycook, M. F. Chisholm, D. E. Jesson, D. P. Norton, D. H. Lowndes, R. Feenstra, and H. R. Kerchner, *Phys. Rev. Lett.* **67**, 765 (1991).